Cell Reports
Article

Endothelial Cells Contribute to Generation of Adult Ventricular Myocytes during Cardiac Homeostasis

Bryan A. Fioret,[1,2] Jeremy D. Heimfeld,[1] David T. Paik,[1] and Antonis K. Hatzopoulos[1,*]
[1]Department of Medicine, Division of Cardiovascular Medicine, and Department of Cell and Developmental Biology, Vanderbilt University, Nashville, TN 37232, USA
[2]Department of Pharmacology, Vanderbilt University, Nashville, TN 37232, USA
*Correspondence: antonis.hatzopoulos@vanderbilt.edu
http://dx.doi.org/10.1016/j.celrep.2014.06.004

SUMMARY

Cardiac tissue undergoes renewal with low rates. Although resident stem cell populations have been identified to support cardiomyocyte turnover, the source of the cardiac stem cells and their niche remain elusive. Using Cre/Lox-based cell lineage tracing strategies, we discovered that labeling of endothelial cells in the adult heart yields progeny that have cardiac stem cell characteristics and express Gata4 and Sca1. Endothelial-derived cardiac progenitor cells were localized in the arterial coronary walls with quiescent and proliferative cells in the media and adventitia layers, respectively. Within the myocardium, we identified labeled cardiomyocytes organized in clusters of single-cell origin. Pulse-chase experiments showed that generation of individual clusters was rapid but confined to specific regions of the heart, primarily in the right anterior and left posterior ventricular walls and the junctions between the two ventricles. Our data demonstrate that endothelial cells are an intrinsic component of the cardiac renewal process.

INTRODUCTION

Classically, the heart has been thought of as a postmitotic organ without intrinsic mechanisms to replace cardiomyocytes (CMs). However, recent studies documented moderate annual CM renewal rates, averaging 0.4%–1% (Bergmann et al., 2009; Murry and Lee, 2009). The origins of cardiac tissue renewal mechanisms have been actively pursued, leading to the identification of several distinct cardiac cell types with stem cell characteristics that have been proposed to contribute to maintenance of the adult mammalian heart (Boudoulas and Hatzopoulos, 2009). One such population consists of cells that form cardiospheres in suspension and differentiate to CMs, endothelial cells (ECs), and smooth muscle cells (SMCs) (Messina et al., 2004; Smith et al., 2007). Cardiac stem cells (CSCs) also include c-Kit expressing cells, which generate CMs, ECs, and SMCs after injury (Beltrami et al., 2003; Rota et al., 2008; Ellison et al., 2013). A different CSC type consists of Side Population (SP) cells (Hierlihy et al., 2002; Martin et al., 2004; Mouquet et al., 2005). The potential of SP cells to differentiate to cardiac cells is higher in the subgroup that expresses stem cell antigen 1 (Sca1) (Pfister et al., 2005). Sca1$^+$ cells independently isolated from adult cardiac tissue express early regulators of cardiac differentiation such as Gata4 and, when stimulated, Nkx2.5 and sarcomeric proteins (Oh et al., 2003). Sca1$^+$ cells home to infarcted myocardium, yielding CMs around the injury area and improving cardiac function (Oh et al., 2003; Wang et al., 2006). Recent transcriptional profiling suggested that c-Kit$^+$ cells represent a less differentiated phenotype, whereas SP and Sca1$^+$ cells are more committed to the cardiac lineage (Dey et al., 2013).

Adult organs, including the brain, gut, bone marrow, and hair follicles, harbor stem cells in specialized niches, allowing for spatial and temporal regulation of the renewal process (Li and Clevers, 2010; Fuentealba et al., 2012). The niche supports quiescent stem cells that upon stimulation give rise to transient amplifying progenitors that differentiate to mature, tissue-specific cell types. However, little is known about the origins of CSCs or the structural organization of the CSC niche in the heart.

We recently showed that after acute ischemic injury in the adult heart, endothelial-to-mesenchymal transition (EndMT) produces bipotent cells that generate both ECs and myofibroblasts during scar formation (Aisagbonhi et al., 2011). Other groups have documented the ability of adult ECs to generate multipotent stem-like cells via EndMT in the bone, demonstrating a degree of EC plasticity and ability to differentiate to alternative cell types (Medici et al., 2010). Based on these findings, we hypothesized that ECs may also contribute to the maintenance of cardiac tissue during homeostasis. Using constitutive and inducible fate-mapping strategies to track cells expressing endothelial genes in the adult mouse heart, we discovered that ECs generate cells with CSC characteristics. EC-derived cells were organized in a radial manner within coronary arteries, with quiescent and proliferative cells residing in the media and adventitia layers, respectively. Distal to the coronary niche, we identified labeled CMs organized in clusters of single-cell origin. EC pulse-chase experiments demonstrated that CM renewal was rapid but spatially restricted. Our data reveal that cells with EC properties are part of the intrinsic cardiac renewal program and that

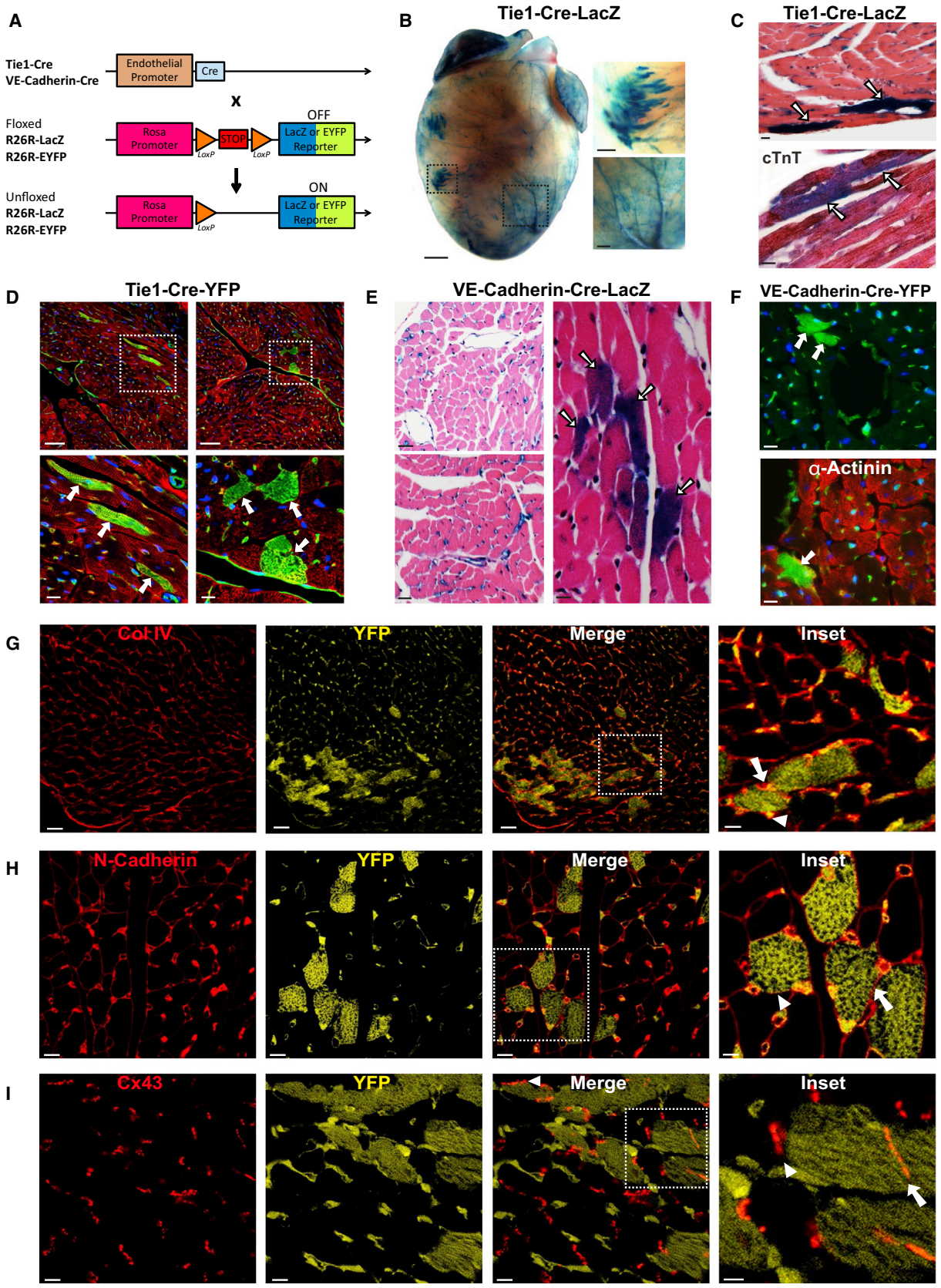

(legend on next page)

coronary arteries constitute a structural component of the cardiac stem cell niche.

RESULTS

Endothelial Fate Mapping Labels CMs in the Adult Heart

To investigate the potential role of the endothelium in maintenance of the normal, uninjured adult heart, we analyzed cell fate in the hearts of 3- to 5-month-old Tie1-Cre-LacZ or Tie1-Cre-YFP mice, which were generated by crossing Tie1-Cre mice to ROSA-β-galactosidase (LacZ) or ROSA-enhanced yellow fluorescence protein (YFP) reporter mice, respectively (Gustafsson et al., 2001; Soriano, 1999; Srinivas et al., 2001) (Figure 1A). In double-transgenic animals, the ubiquitous *Rosa26* promoter constitutively drives reporter gene expression in ECs and their progeny.

Tie1-Cre-LacZ hearts were stained with X-gal to visualize β-galactosidase (β-gal) activity and thus Tie1$^+$ cells and their derivatives. In addition to labeled ECs as expected, we observed X-gal$^+$ cells of nonendothelial appearance that were organized in clusters (Figure 1B). Histological analysis showed that the β-gal$^+$ clusters were CMs, based on morphology and costaining for cardiac Troponin T (Figure 1C). To exclude that CM staining was due to aberrant β-gal activity in CMs, we stained cardiac tissue sections from Tie1-Cre-YFP mice with antibodies that recognize YFP and the CM marker α-Actinin. Immunofluorescence (IF) analysis showed robust EC staining, but also revealed the presence of YFP$^+$ CMs with proper sarcomeric structures (Figure 1D). EC-derived CMs in sections appeared in clusters, in agreement with the pattern observed in whole-mount images.

To eliminate the possibility that CM staining was due to ectopic Tie1 promoter activity in cardiac cells, we used mice expressing *β-gal* directly under the Tie1 promoter to mark ECs, but not their progeny (Korhonen et al., 1995). Histological analysis at 2 days, 2 weeks, 1 month, and 2 months of age detected exclusive EC labeling, without β-gal$^+$ CMs (Figure S1). These results indicate that the labeled CMs observed in Tie1-Cre-LacZ and Tie1-Cre-YFP hearts were progeny of Tie-1$^+$ cells and not due to ectopic Tie1 expression in CMs.

To further confirm that ECs give rise to CMs, we used an independent mouse line with endothelial-specific Cre expression under the control of the *vascular endothelial (VE)-cadherin* gene transcription regulatory elements (Alva et al., 2006) (Figure 1A). The VE-Cadherin promoter-based labeling produced results comparable to those obtained with the Tie1-Cre-LacZ or Tie1-Cre-YFP mice. Specifically, histological sections obtained from 3- to 5-month-old VE-Cadherin-Cre crossed to ROSA-LacZ (VE-Cadherin-Cre-LacZ) or ROSA-YFP (VE-Cadherin-Cre-YFP) hearts showed labeling of both ECs and CMs (Figures 1E and 1F).

IF analysis showed that EC-derived, YFP$^+$ CMs were surrounded by normal basal membrane (Collagen IV staining), properly expressed cell-adhesion membrane molecules (N-Cadherin), and formed gap junctions (Connexin 43) among themselves as well as with non-EC-derived CMs, suggesting that they are functionally integrated with neighboring YFP$^-$ CMs (Figures 1G–1I). Taken together, our results show that in adult mice, fate mapping using endothelial genetic labeling yields cells with the functional and structural properties of CMs.

Endothelial-Derived Myocytes First Appear 2 Weeks after Birth

During development, mesodermal progenitor cells, which differentiate to ECs, CMs, and SMCs, also express the endothelial-specific gene *vascular endothelial growth factor receptor 2* (*Vegfr2*; Kattman et al., 2006). This raised the possibility that the labeled CM clusters in the adult heart were derived from early embryonic cells with endothelial characteristics. To distinguish whether the EC-derived CMs were of embryonic or adult origin, we used End-SCL-CreER^T mice with inducible Cre recombinase expression under the control of the 5′ endothelial-specific enhancer of the *stem cell leukemia* (*SCL*) gene (Göthert et al., 2004). End-SCL-CreER^T mice were crossed to the ROSA-LacZ or ROSA-YFP reporter lines to generate End-SCL-CreER^T-LacZ or End-SCL-CreER^T-YFP mice, respectively. These double-transgenic mice allow for specific labeling of mature ECs after tamoxifen induction of Cre-recombinase activity.

End-SCL-CreER^T-LacZ and End-SCL-CreER^T-YFP adult mice were continuously fed a diet containing 0.8% tamoxifen to tag and lineage trace ECs. Whole-mount staining with X-gal and histological analysis of End-SCL-CreER^T-LacZ hearts after 6 weeks of the tamoxifen diet showed EC as well as CM labeling (Figures

Figure 1. Lineage Tracing of EC Fate Leads to CM Labeling in the Adult Heart

(A) Schematic drawing of the gene loci used for EC lineage tracing and fate mapping.

(B) Whole-mount X-gal staining of hearts from 3-month-old Tie1-Cre-LacZ mice shows EC labeling and clusters of non-ECs in the ventricles. Right panels represent boxed areas showing a cluster of labeled non-ECs (upper panel) and ECs (lower panel). Scale bars, 1 mm in original image, 250 μm in insets.

(C) Upper panel: histological analysis of X-gal-stained cardiac tissue sections from Tie1-Cre-LacZ mice shows CM staining (arrows). Lower panel: labeled non-ECs costain for cardiac Troponin T (cTnT; arrows). Scale bars, 10 μm.

(D) IF analysis of cardiac tissue from Tie1-Cre-YFP mice stained for YFP (green) shows ECs and CMs, with the latter costained for α-Actinin (red). YFP$^+$ CMs (arrows) are shown sectioned longitudinally (left) and transversely (right). DAPI (blue) was used for nuclear counterstaining. Lower panels depict boxed areas to showcase sarcomeric structures in YFP$^+$ CMs. Scale bars, 50 μm (top panels) and 10 μm (bottom panels).

(E) Histological analysis of X-gal-stained cardiac tissue from VE-Cadherin-Cre-LacZ mice shows staining of ECs (left panels). A labeled CM cluster is highlighted in the right image. Scale bars, 25 μm (left panels) and 10 μm (right panel).

(F) IF analysis of cardiac tissue from VE-Cadherin-Cre-YFP mice costained for YFP (top and bottom, green) and α-Actinin (bottom; red). DAPI (blue) was used for nuclear counterstaining. Scale bars, 10 μm. See also Figure S1.

(G–I) IF analysis of cardiac tissue from Tie1-Cre-YFP mice indicating YFP (yellow) and basal membrane Collagen IV (G; Col IV, red), membrane cell adhesion protein N-cadherin (H, red), and gap junction protein Connexin 43 in intercalated discs (I; Cx43, red). YFP antibody marks both ECs and EC-derived CMs. Higher-magnification insets are shown in the right panels. Arrows indicate adjacent YFP$^+$/YFP$^+$ CMs; arrowheads indicate adjacent YFP$^+$/YFP$^-$ CMs. Scale bars, 30 μm (G) and 10 μm (H and I) in original images, and 10 μm (G) and 5 μm (H and I) in insets.

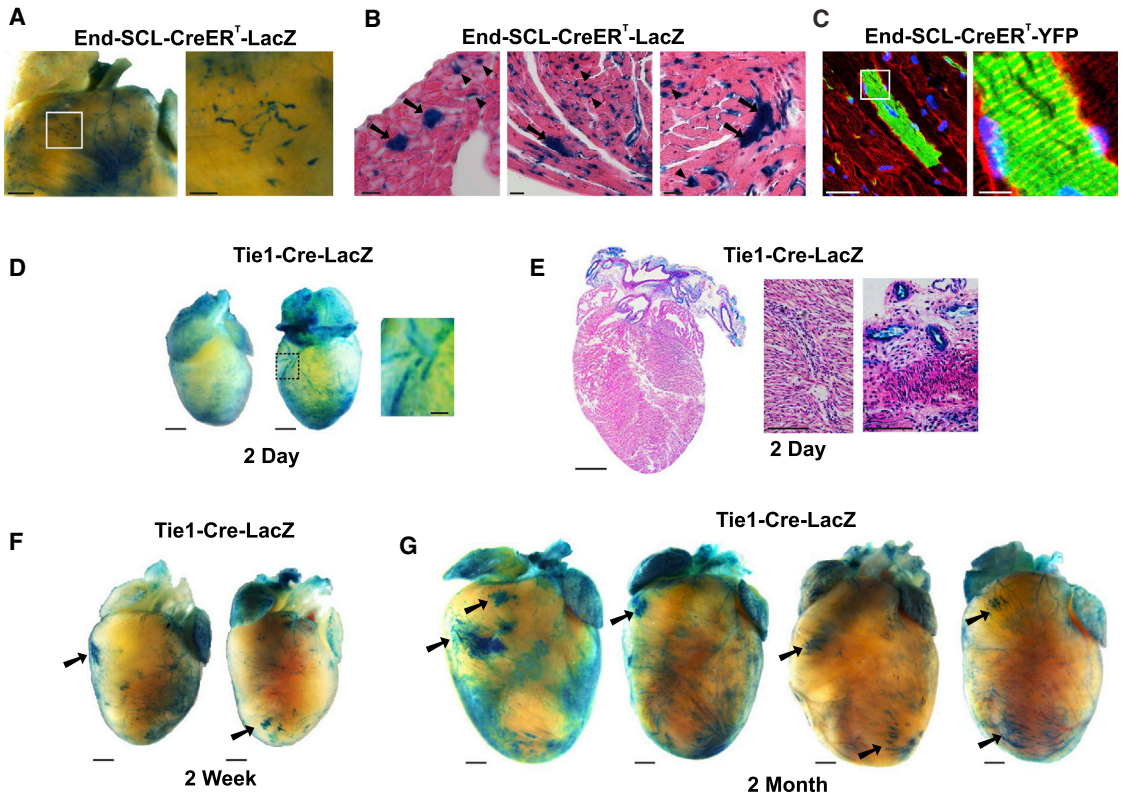

Figure 2. Endothelial-Derived CMs Appear in the Adult Heart

(A and B) Images of X-gal-stained hearts from 5-month-old End-SCL-CreER^T-LacZ mice that were fed tamoxifen chow for 6 weeks to induce Cre recombinase in adult ECs and their progeny. Whole-mount staining in (A) shows EC and CM labeling. Scale bar, 1 mm in original image, 250 μm in inset. Histological sections in (B) depict labeled CMs (arrows) and ECs (representative arrowheads). Scale bars, 20 μm.

(C) Labeling of cardiac ECs and CMs in the End-SCL-CreER^T-YFP double-transgenic line after 12 weeks of the tamoxifen diet. Sections stained for YFP (green) and α-Actinin (red). Right panel: magnification of the boxed area highlights sarcomeric structures in YFP$^+$ CM. Scale bars, 10 μm (left) and 5 μm (right).

(D and E) Whole-mount images (D) and sections (E) of X-gal-stained neonatal hearts from 2-day-old Tie1-Cre-LacZ mice shows EC, but not CM, labeling. Scale bars, 1 mm in original images, 250 μm in magnified areas.

(F and G) X-gal staining of hearts from weanling (2-week-old) and young adult (2-month-old) mice shows that EC-derived CM clusters appear at ~2 weeks of age. Scale bars, 1 mm.

See also Figure S2.

2A and 2B), similar to the constitutively active endothelial-specific Cre models described in Figure 1. Labeling of CMs, which costained for sarcomeric α-Actinin, was also observed after 12 weeks on tamoxifen (Figure 2C). Of note, we did not detect CM labeling and found extremely rare EC labeling (<1%) in control End-SCL-CreER^T-LacZ mice without tamoxifen administration, indicating tight regulation of inducible Cre recombinase activity. No labeled cells were present in ROSA-STOP-LacZ mice on tamoxifen (Figure S2).

To test whether the observed CM staining was due to ectopic activity of the Tie1 or Endothelial-SCL promoter/enhancer elements in non-ECs, we stained cardiac tissue sections from Tie1-Cre-YFP and End-SCL-CreER^T-YFP mice with antibodies that recognize Cre protein. IF analysis showed that Cre expression was restricted to ECs, supporting an endothelial origin of labeled CMs (Figure S2). We confirmed the endothelial specificity of Tie1 expression by costaining cardiac sections from Tie1-Cre-YFP mice for Tie1 and α-Actinin. We did not detect colabeling of Tie1 in YFP$^+$ or YFP$^-$ CMs, showing that CMs do not express Tie1 (Figure S2). Collectively, these results indicate that the observed labeling was not due to leaky activity of the inducible Cre fusion protein, expression of β-gal and YFP without Cre activity, or aberrant Tie1 or Cre expression in CMs.

To further exclude the possibility that the EC-derived CMs were marked during development, we isolated and X-gal stained hearts from neonatal and young Tie1-Cre-LacZ mice. Staining of hearts from perinatal day 2 (P2), weanling (P14), and young adult (2-month-old) mice indicated that while the cardiac vasculature was labeled at each time point (Figures 2D–2G), CM clusters first appeared within the postnatal heart by 2 weeks of age (Figures 2F and 2G).

In brief, we used three independent, constitutive (Tie1 and VE-Cadherin) or inducible (End-SCL) endothelial-specific promoters and two independent reporters (LacZ and YFP), all of which showed similar labeling of ECs and CM clusters. Thus,

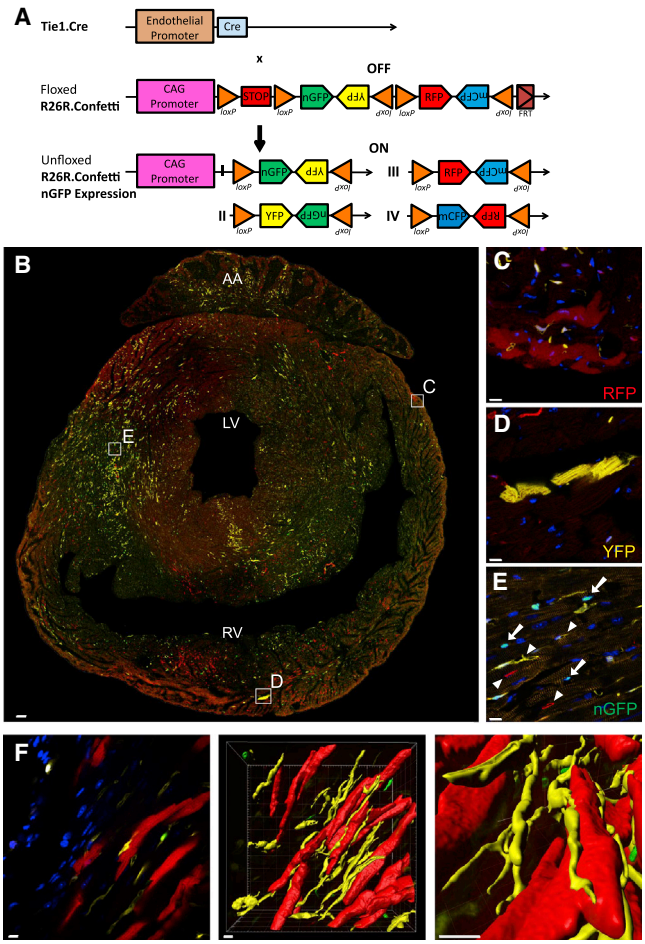

Figure 3. Endothelial-Derived CMs Are of Clonal Origin

(A) Schematic drawing of the ROSA-Confetti reporter gene locus.

(B–E) Epifluorescence analysis for RFP, YFP, and nGFP expression in transverse cardiac sections from adult Tie1-Cre-Confetti mice depicts ECs and CMs expressing RFP, YFP, and nGFP. CM clusters marked in the boxed areas in (B) are magnified in (C)–(E). Individual CMs in each cluster express the same fluorescent protein. Scale bars, 100 μm in (B) and 10 μm in (C)–(E).

(F) 3D reconstruction of a representative CM cluster (each CM expressing RFP) and adjacent ECs expressing YFP. Scale bars, 10 μm.

See also Figure S3.

our data support the idea that a subset of CMs in the adult mouse heart are postnatally derived from ECs.

Clusters of Endothelial-Derived CMs Originate from Single Cells

The clustering of EC-derived CMs suggested they were clonally related. To test this model, we crossed the Tie1-Cre line to the ROSA-Confetti multifluorescent reporter to generate Tie1-Cre-Confetti mice. The Confetti line carries four distinct fluorescent protein genes (red, yellow, nuclear green, and membrane-bound cyan) in the ROSA locus (Snippert et al., 2010). The fluorescent protein coding sequences are organized in tandem among alternating LoxP sites in such a way that recombination of the ROSA-Confetti allele leads to stochastic expression of RFP, YFP, nuclear GFP (nGFP), or membrane CFP (mCFP). The construct is designed such that random recombination activates only one of the fluorescent protein genes, allowing stochastic labeling of each targeted cell and its descendants with a single color (Figure 3A). As a result, this fate-mapping strategy can distinguish whether cells in a cluster are clonally related (i.e., generated from a single, labeled progenitor cell) or if each cell in a cluster has been independently derived. In the first case, the entire cluster should have CMs of one color; if the latter is true, individual clusters should consist of cells expressing different colors (Greif et al., 2012).

Epifluorescence examination of cardiac sections from adult Tie1-Cre-Confetti mice detected ECs expressing RFP, YFP, and nGFP in equal proportions (Figure S3) (in our hands, expression of mCFP in cardiac sections was too weak to reliably detect; therefore, we focused further analysis on RFP, YFP, and nGFP). Among labeled CMs, each individual cluster was marked by expression of the same single fluorescent protein (Figures 3B–3E). To calculate the probability (p) that each cluster would randomly consist of CMs expressing the same fluorescent protein *without* being derived from a single cell, we recorded the size and color of CM clusters with three or more cells in sections of three independent Tie1-Cre-Confetti mouse hearts (Figure S3). The probability that the observed labeling patterns in this analyzed set of CMs are due to random recombination events is $p < 10^{-36}$, indicating that labeled CMs in each cluster are not independently derived, but originate from a single cell.

Using 3D reconstruction images, we documented that in many instances individual CM clusters were marked by a different fluorescent color than the neighboring microvasculature, suggesting that the CM labeling was not due to fusion with ECs (Figure 3F). Furthermore, CMs in the same cluster were not always contiguous and often were interspersed with unlabeled CMs. This pattern is also observed in other organs and might be indicative of tissue repair in the adult rather than de novo development in the embryo (Kopinke et al., 2011; Bowman et al., 2013). Collectively, the staining patterns in Tie1-Cre-Confetti mice indicate that each labeled CM cluster originated from a single parental cell expressing EC markers. It is also possible that rare, proliferating CMs transiently express endothelial markers and thus become labeled before they expand to form clusters.

Cardiac Myocyte Progeny of ECs Are Regionally Restricted

Whole-mount heart staining indicated that EC-derived CM clusters were localized in specific areas (Figures 1B, 2F, and 2G). To determine overall distribution patterns throughout right and left ventricles, we systematically mapped the location of CM progeny following EC lineage tracing. We analyzed complete sets of serial transverse cardiac tissue sections from five Tie1-Cre-YFP mice using confocal microscopy. The results revealed that clusters of labeled CMs were present in both the left and right ventricles, most frequently around coronary blood vessels in subepicardial regions (Figures 4A and 4B). The locations of clusters containing four or more YFP^+ CMs were placed in a diagram of four heart planes from base to apex. We found that YFP^+ CM clusters were primarily localized in three regions of the heart: the anterior free wall of the right ventricle, the junction areas between

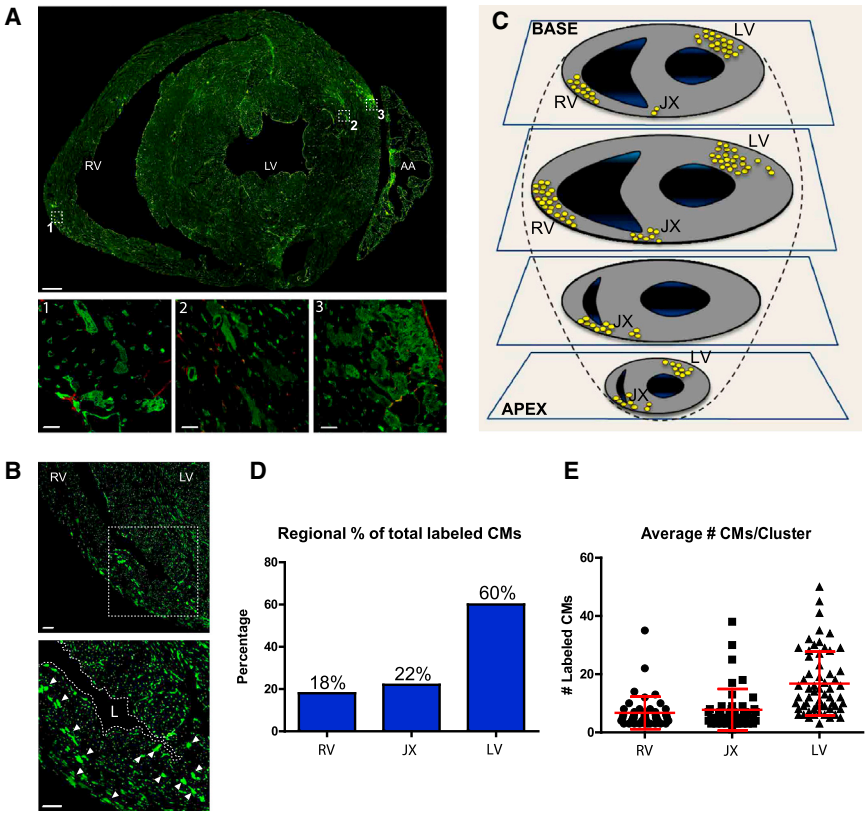

Figure 4. Endothelial-Derived CMs Are Localized to Three Specific Heart Areas

(A) A transverse cardiac section from adult Tie1-Cre-YFP mice stained for YFP reveals that EC-derived YFP$^+$ CMs are found in both the left and right ventricles, most frequently in perivascular (insets 1–3) and subepicardial (insets 1 and 3) areas. Scale bars, 500 μm in original image and 10 μm in insets.

(B) Clusters of CMs are also localized at the junction of the left and right ventricles and adjacent septum. Scale bars, 50 μm.

(C) Schematic drawing depicting the location of all clusters of four or more YFP$^+$ CMs identified in serial sections of five Tie1-Cre-YFP mice.

(D) Quantification of CM cluster locations shows that 60% are present in the left ventricle and the remaining 40% are present in the right ventricle and junction areas.

(E) Quantification of the number of CMs in each cluster shows that on average, clusters in the left ventricle have twice as many CMs as those in the right ventricle. AA, atrial appendage; RV, right ventricle; LV, left ventricle; JX, junction; L, lumen.

the right and left ventricles and adjacent septum, and the lateral free posterior wall of the left ventricle (Figure 4C).

Each cluster consisted of up to 50 CMs; 60% of the observed clusters were in the left ventricle and the remaining 40% were equally distributed in the right ventricle and junction areas. Furthermore, on average, the left-ventricle clusters consisted of twice as many cells per cluster compared with those in the right ventricle (Figures 4D and 4E). Taking into account the number of clusters in each heart and the number of cells per cluster, we calculated that the total number of YFP$^+$ CMs represent ~0.3% of the ~8 million CMs in the mouse heart (Adler et al., 1996; Doevendans et al., 1998). These data indicate that in both ventricles, the cardiogenic endothelium seeds specific cardiac areas, representing a relatively small fraction of the CM population.

Pulse Labeling of ECs Leads to Rapid Long-Term CM Labeling

To test whether ECs are the originating cells or represent an intermediate, transient step in the cardiogenic process, we pulse-chased ECs using the inducible End-SCL-CreER^T-LacZ mouse described above. Adult mice were given a series of closely spaced tamoxifen injections ("pulse") and hearts were isolated at various time points after the final injection ("chase") (Figure 5A). Their hearts were then stained with X-gal to visualize labeled CMs in transverse sections. Analysis of cardiac tissue sections immediately (i.e., 1 day after the end of the pulse) and 3 days later showed exclusive labeling of ECs, whereas labeled CMs appeared 1 week after the pulse and persisted up to 12 weeks, the last time point examined (Figure 5B).

The number of labeled CMs per volume of cardiac tissue was quantified for each time point. The data indicate that labeled CMs appeared in low numbers 1 week after the pulse, increased over a period of 3 weeks, and remained relatively constant for at least up to 12 weeks (Figure 5C). These results suggest that cells labeled by EC-specific Cre expression represent an originating cell rather than a transient subpopulation in the CM generation process, since in the latter case CM numbers would decline after a single pulse. Alternatively, it is likely that EC-derived CMs have long lifespans beyond the examined 12-week period. In either case, the duration required to achieve maximum CM labeling after the pulse suggests the process is rapid and reaches a steady state within ~3 weeks.

SCL, Tie1, and VE-Cadherin are also expressed in hematopoietic stem cells (HSCs), raising the possibility that the labeled CMs are of bone marrow origin. One advantage of the SCL 5′ enhancer is that it is not expressed in adult HSCs (Göthert et al., 2004), which suggests that labeled CMs are derived from ECs and not bone marrow cells. To directly test whether HSCs contribute CMs in the adult heart, we used a method that is independent of lineage tracing. Specifically, we analyzed cardiac tissues from mice transplanted with fluorescently tagged bone marrow cells (Figure S4). IF analysis showed that bone-marrow-derived cells present in the adult heart were primarily F4/80$^+$ macrophages and FSP-1$^+$ fibroblasts, with no labeling of CMs, consistent with previous studies (Murry et al., 2004). The results of the transplantation studies excluded the possibility that the labeled CM clusters were derived from HSCs.

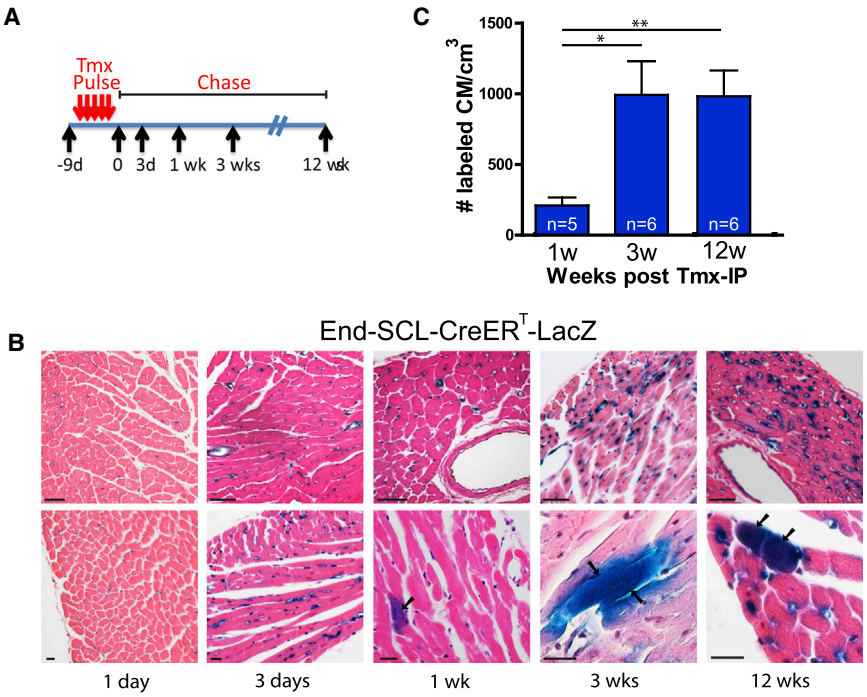

Figure 5. Pulse-Chase Labeling of ECs Leads to Rapid Long-Term Labeling of CM Progeny

(A) Schematic drawing of the pulse-labeling experimental design.

(B) Histological analysis of hearts stained with X-gal and counterstained with H&E to visualize ECs and labeled CMs in transverse sections at the indicated time points. After 1- and 3-day chases, labeling of only cardiac ECs was observed, whereas labeled CMs appeared by 1 week after the pulse and persisted at 3 months. Arrows indicate X-gal$^+$ CMs. Scale bars, 50 μm (upper) and 20 μm (lower panels).

(C) Quantification of CM numbers at different chase time points shows maximum CM labeling within 3 weeks, which remains constant thereafter (n, number of mice used for analysis). Values reported as mean ± SD; *$p < 0.05$, **$p < 0.01$.

See also Figure S4.

Endothelial Fate Mapping Identifies Quiescent and Proliferating Perivascular Cells Expressing Early Cardiac Markers

The above results indicate that ECs represent an originating source of CMs rather than a transient cell type. This model predicts that EC lineage tracing will mark intermediate, proliferating cell populations that express early cardiac markers but have not yet differentiated to CMs.

In support of this model, an examination of cardiac tissue sections obtained from Tie-Cre-YFP, Tie-Cre-LacZ, and End-SCL-CreER^T-LacZ mice revealed that besides ECs and CMs, EC fate mapping marked two additional cell types (Figures 6A, 6B, and S5A–S5C). The first resided in the media layer of coronary arteries and was marked by expression of α smooth muscle actin (αSMA) (Figure 6A). YFP$^+$/αSMA$^+$ double-positive cells in the media layer of coronary vessels, termed M cells, also expressed the early cardiac transcription factor Gata4, but lost expression of the EC marker CD31 (arrow, Figure 6B). Serial histological analysis revealed that half of the coronary artery sections had M cells, which constituted approximately 27% of the SMC population in those coronary arteries. Moreover, 44% of the YFP$^+$/αSMA$^+$ M cells expressed nuclear Gata4 protein (Figure 6C).

The second subpopulation, termed A cells, was found within or immediately adjacent to the adventitia layer of coronary vessels (Figures 6B and 6E–6G). Approximately half of the coronary arteries had A cells, and nearly 65% of them expressed Gata4 (Figures 6B, 6D, and S5A). The A cells did not express EC markers, as indicated by the absence of CD31 expression, and were also negative for mature CM markers such as α-Actinin (Figures 6E and 6F). The A cells were often small in size and found in clusters that stained with antibodies recognizing the cell-cycle markers Ki67 and phospho-Histone H3 (pH3) (Figures 6F and 6G). Approximately 20% of A cells stained positive for proliferation markers (Figure 6H). The proliferative phenotype was a unique property of A cells among all labeled cell types identified in the cell-fate-mapping experiments.

Furthermore, lineage tracing using Tie1-Cre-Confetti mice indicated that coronary ECs and M cells were heterogeneously labeled and expressed different-colored fluorescent proteins (Figures 6I and 6J). In contrast, A cell clusters were uniformly marked by the same color of fluorescent protein, suggesting that A cell clusters expand from a single cell, consistent with their expression of proliferation markers (Figures 6J and S5D). Pulse-chase analysis of ECs using the inducible End-SCL-CreER^T-LacZ mouse showed that EC-derived perivascular M and A cells could be detected as early as 3 days after the end of the tamoxifen pulse (Figure S5C).

IF analysis showed no Cre recombinase protein expression in labeled M and A cells, supporting an endothelial origin (Figure S5E). Consistent with this possibility, staining of heart tissue sections from Tie1-Cre-YFP and wild-type C57Bl/6 mice with antibodies recognizing mesenchymal markers illustrated that a rare subpopulation of coronary endothelium, representing ~2.5% of coronary ECs, expresses the mesenchymal marker FSP-1 (Zeisberg et al., 2007) as well as proteins that are known to initiate mesenchymal transformation, such as Snail (Timmerman et al., 2004) (Figures 6K, 6L, S5F, and S5G). Subcellular Snail localization was observed in both nuclear and cytoplasmic compartments, a pattern that depends on the activation state of Snail (Domínguez et al., 2003). These data lend support to the idea that labeled perivascular cells of EC origin are derived by EndMT.

Endothelial Progeny in Perivascular Areas include Sca-1$^+$ Cardiac Progenitor Cells

The results of the lineage tracing experiments and the identification of EC-derived intermediate cell populations suggested that

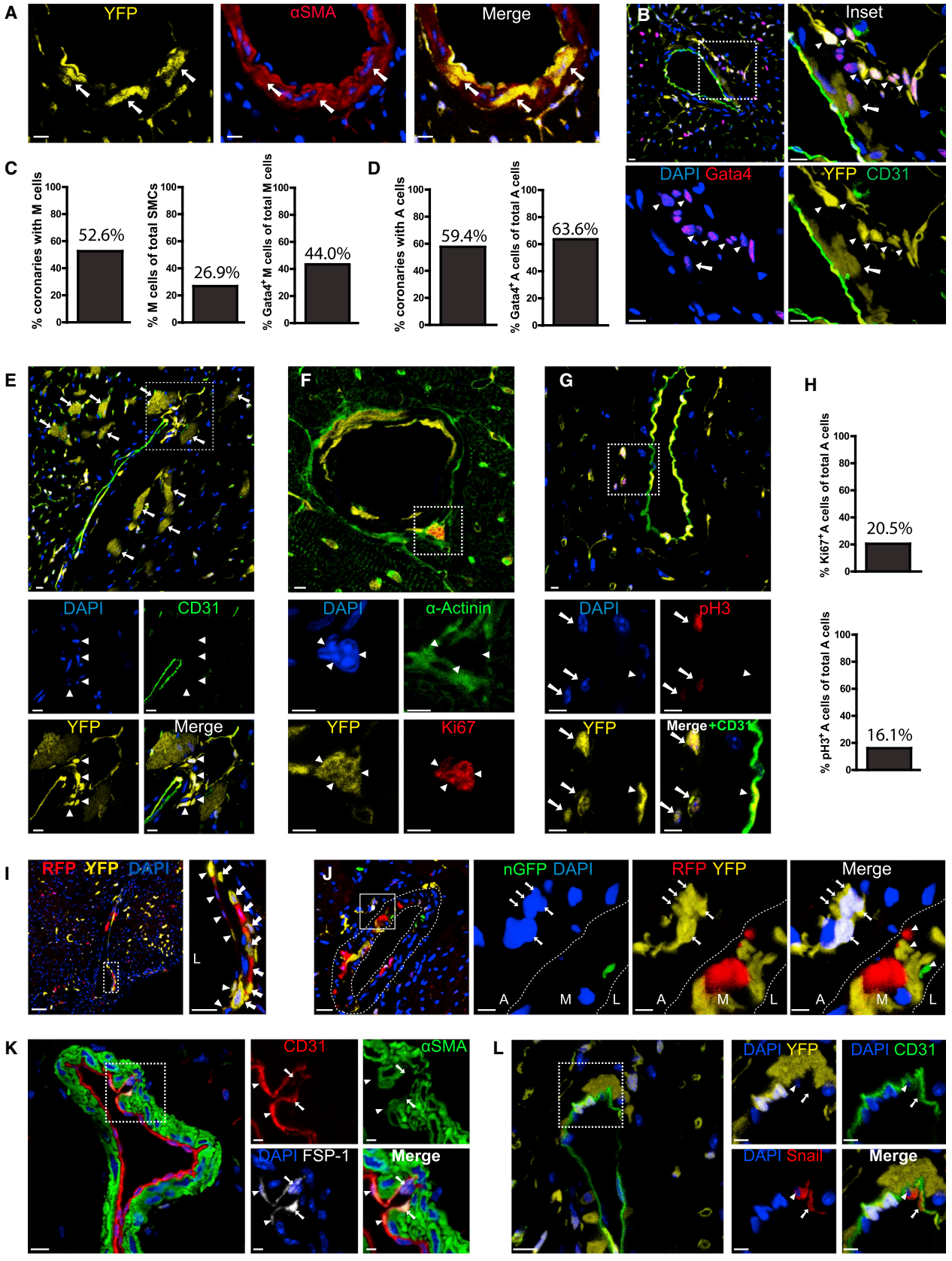

(legend on next page)

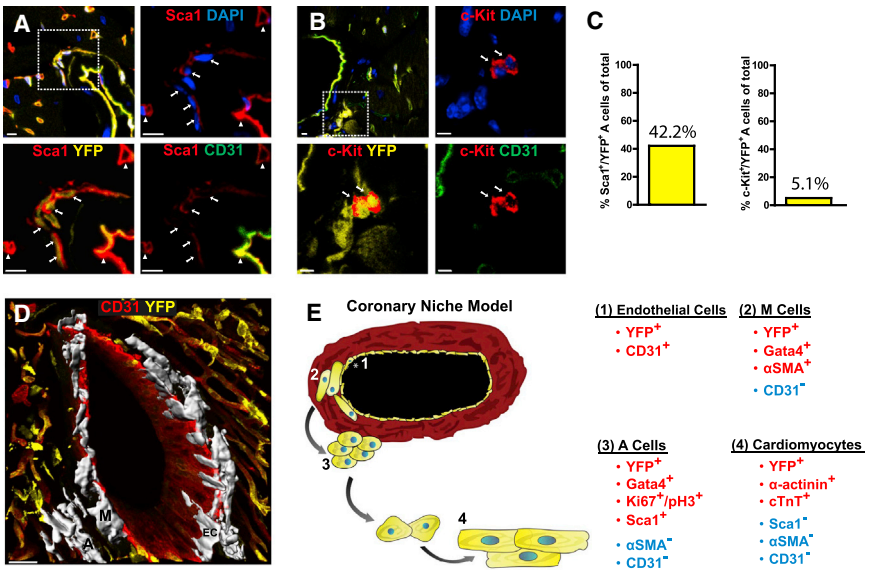

Figure 7. Endothelial Fate Mapping Yields Cardiac Progenitor Cells

(A and B) IF analysis of cardiac tissue sections from Tie1-Cre-YFP mice reveals that YFP$^+$/CD31$^-$ A cells express Sca1 (A), whereas a small subpopulation expresses c-Kit (B). Arrows in magnified areas in (A) indicate YFP$^+$/Sca1$^+$ cells, and arrowheads indicate Sca1$^+$ ECs. Arrows in (B) indicate cKit$^+$ cells in magnified areas. DAPI was used for nuclear counterstaining. Scale bars, 5 μm.

(C) Serial section analysis of cardiac tissue shows that ~40% and 5% of A cells are Sca1$^+$ or c-Kit$^+$, respectively.

(D) 3D reconstruction illustrates endothelial-derived M and A cells (highlighted in white; representative cells are marked by M and A, respectively) within the coronary niche. EC indicates coronary ECs. Scale bar, 30 μm.

(E) Schematic drawing of the cardiac stem cell niche model illustrates the spatial organization of EC progeny and their corresponding expression profiles.

See also Figure S6.

these intermediates represent cardiac progenitor cells. To test this possibility, we stained cardiac tissue sections from Tie1-Cre-YFP mice with antibodies recognizing Sca1 and c-Kit, two established cell-surface markers of CSCs. The results showed that M cells did not express either marker. However, 42% of the YFP$^+$ A cells stained positive for Sca1, whereas only a small subset (5%) of A cells stained positive for c-Kit (Figures 7A–7C). Further histological analysis showed that the majority (>70%) of perivascular, Sca1$^+$/CD31$^-$ cells expressed YFP. These results suggest that a significant fraction of Sca1$^+$ CSCs are descendants of ECs. 3D reconstruction of a coronary artery, using z-stack imaging, provided a physical depiction of the spatial arrangement of M and A cells within the coronary niche (Figures 7D and S6).

Considering the results described above and taking into account the cellular spatial relationships (i.e., the distance from the coronary endothelium), we propose the following model (Figure 7E): endothelial or endothelial-like cells give rise to quiescent, perivascular cells in the coronary wall that lose EC markers and acquire SMC characteristics. These cells, termed M cells, express early cardiac differentiation markers such as Gata4. Further distal to the vascular wall, M cells are replaced by A cells, which lose SMC characteristics but maintain expression of Gata4, and acquire markers of CSCs such as Sca1$^+$. The A cells

Figure 6. Endothelial Fate Mapping Yields Two Distinct Types of Perivascular Cells

(A–G) IF analysis of cardiac tissue sections from Tie1-Cre-YFP mice.

(A) YFP$^+$/αSMA$^+$ cells (termed M cells) are present in the media layer of coronary arteries (arrows). Scale bars, 10 μm. DAPI was used for nuclear counterstaining in these and subsequent IF images.

(B) YFP$^+$/CD31$^-$ cells (termed A cells) are present within or immediately adjacent to the adventitia layer of coronary vessels. The magnification inset shows that both M (arrows) and A (arrowheads) cells acquire expression of Gata4 protein (see also Figure S5A). Scale bars, 10 μm.

(C) Quantification using cardiac tissue serial sections reveals that 52.6% of the coronary arteries contain EC-derived M cells (left graph). In these coronaries, ~27% of SMCs are EC-derived M cells (middle) and 44% of the M cells express Gata4 (right).

(D) Quantification using serial sections reveals that approximately half of the coronary arteries contain endothelial-derived A cells (left graph) and ~65% of the A cells express Gata4 (right).

(E) A cells are often found in close proximity to YFP$^+$ CMs (arrows). YFP$^+$ A cells lost CD31 expression (arrowheads in magnified boxed areas below). Scale bars, 10 μm.

(F) A cells (arrowheads in magnified boxed area) do not express α-Actinin, but stain positive for the proliferation marker Ki-67.

(G) A cells (arrows in magnified boxed area) stain positive for the proliferation marker pH3. Arrowheads indicate YFP$^+$ ECs. Scale bars, 5 μm.

(H) Ki-67$^+$ (top graph) and pH3$^+$ (bottom) cells represent ~20% and 16% of A cells, respectively.

(I and J) Epifluorescence analysis of cardiac sections from Tie1-Cre-Confetti mice.

(I) Images show heterogeneous labeling of M cells expressing either RFP or YFP (arrows). Arrowheads indicate RFP$^+$ or YFP$^+$ ECs. Scale bars, 50 μm for original and 20 μm for inset.

(J) Clusters of A cells are uniformly marked by a single color of fluorescent protein (YFP). In the magnified area, arrows point to YFP$^+$ A cells. Heterogeneous labeling of fluorescent M cells (with RFP, YFP, or nGFP) is seen in the media layer (arrowheads, merge). Scale bars, 20 μm for original and 5 μm for insets.

(K) IF analysis of cardiac sections from C57Bl/6 mice stained for CD31 (red), αSMA (green), and FSP-1 (white) indicates a rare population of CD31$^+$/FSP1$^+$ ECs.

(L) Cardiac sections from Tie1-Cre-YFP mice show that a subpopulation of coronary ECs express Snail. Arrowheads indicate nuclear costaining; arrows indicate cytoplasmic costaining. Scale bars, 10 μm for originals and 5 μm for insets. L, M, and A in (I) and (J) insets stand for lumen, media, and adventitia, respectively, of the coronary arterial wall.

See also Figure S5.

proliferate, leave the coronary niche, and differentiate to CMs. Thus, EC-derived YFP$^+$ M and A perivascular cells within the medial and adventitial layers of coronary vessels likely serve as intermediate populations during generation of adult CMs.

Although the proposed model is consistent with the observed data, alternative interpretations may also explain the pattern of the lineage tracing results. For example, low-level expression of endothelial genes in cardiac fibroblasts with cardiogenic potential could account for some of the observed labeling patterns. Or, as mentioned above, rare proliferating CMs may transiently express endothelial genes and thus become labeled before expansion occurs. Although we did not observe expression of endothelial markers in fibroblasts and CMs, we cannot fully exclude these possibilities.

DISCUSSION

Current evidence showing low rates of CM apoptosis suggests that a renewal mechanism is required to maintain cardiac tissue (Anversa et al., 2006; Ellison et al., 2007), yet there is little information regarding the native regenerative mechanisms that function during cardiac homeostasis. We used Cre/Lox technology to generate a fate map of vascular cells in the healthy, adult heart. Our data show that (1) ECs retain cardiogenic potential in the adult heart, similar to the differentiation capacity of cardiovascular progenitor cells during the early stages of cardiac development; (2) the EC-based cardiogenic process is rapid but restricted to specific areas of the myocardium; (3) ~0.3% of the adult heart is comprised of endothelial-derived CMs; (4) the EC-based regenerative mechanism generates both quiescent (M cells) and proliferative (A cells) progeny expressing early-stage cardiac differentiation genes such as Gata4; (5) Sca1$^+$ cardiac stem cells are EC progeny; and (6) the coronary arteries serve as a structural component of the cardiac stem cell niche.

Although the classical role of ECs is to ensure proper functioning of the inner wall in blood vessels, increasing evidence indicates that they have exceptional differentiation potential and plasticity, and thus play a more direct role in organ development, homeostasis, and repair. During development, for example, hemogenic endothelia in the ventral wall of the dorsal aorta transform into budding blood cells and migrate to hematopoietic organs, ultimately residing in the bone marrow (Lancrin et al., 2009). In the adult, besides the angiogenic response of ECs to build new blood vessels after ischemia, they also undergo EndMT after injury, producing SMA$^+$ myofibroblasts in the heart, lung, and kidney, supporting a fibrogenic potential of ECs (Zeisberg et al., 2007, 2008; Arciniegas et al., 2007; Aisagbonhi et al., 2011; Chen et al., 2012).

Our results indicate that ECs also have cardiogenic potential in the adult. This notion is compatible with embryonic development when all three types of cardiovascular cells (ECs, SMCs, and CMs) are derived from multipotent progenitor cells expressing EC markers such as Vegfr2 (Kattman et al., 2006). Furthermore, inactivation of SCL/TAL1 can transform vasculature to cardiac cells, turning the yolk sac from a hematopoietic tissue to a contracting sheet of CMs (Van Handel et al., 2012). This striking outcome suggests that, at least early in development, the EC-to-CM transition can be accomplished by switching off a single transcriptional regulator.

Collectively, the data obtained here during cardiac homeostasis and previous data showing that ECs contribute to angiogenesis and fibrosis after injury indicate that ECs remain multipotent in the adult. However, it is not clear whether this is a universal property of mature cardiac ECs or is confined to specific EC subpopulations within coronary arteries. It is also likely that a multipotent cardiovascular stem cell expressing EC markers exists in the adult and is genetically labeled by EC lineage tracing approaches. Finally, the cardiogenic endothelium may represent one mechanism of cardiac regeneration, but our findings do not exclude the possibility of alternative sources of CSCs or the proliferation of resident CMs (Senyo et al., 2013; Malliaras et al., 2013).

Our data provide evidence that the majority (>70%) of Sca1$^+$ CSCs are derived from cells with endothelial characteristics. EC-derived Sca1$^+$ cells expressed early cardiac markers such as Gata4, but lacked mature CM characteristics such as sarcomeric structures and α-Actinin expression. Interestingly, lineage tracing of Sca1$^+$ CSCs showed that they give rise to myocardial cells in the adult heart (Uchida et al., 2013). We found limited overlap between endothelial-derived YFP$^+$ cells and c-Kit$^+$ cells, by contrast, suggesting that the majority of c-Kit$^+$ cells in the heart belong to a different lineage.

An important result of EC lineage tracing during cardiac homeostasis is the emergence of the coronary arteries as the site of the CSC niche. Previous studies showed that the vasculature is an integral component of most well characterized stem cell niches in various organs, such as the bone marrow and the subventricular zone (SVZ) in the brain (Li and Clevers, 2010; Fioret and Hatzopoulos, 2014). Our data suggest that this biological strategy extends to the heart, with the coronary vessels serving as the CSC niche. In support of this finding, vascular progenitor cells have been observed in the walls of coronary arteries in the human heart (Bearzi et al., 2009).

Moreover, our data show that EC-derived Gata4$^+$ cells around the coronary arteries can be divided into subpopulations based on several criteria (location, size, molecular markers, and proliferation status), indicating the CSC niche is organized in a radial manner with the vasculature at the center. M cells, which are closest to the lumenal ECs, are quiescent and combine smooth muscle and early cardiac characteristics, whereas A cells farther afield in the adventitia are proliferative and acquire expression of Sca1. In many respects, the CSC niche shares similarities with the neuronal stem cell niches in the brain. Here, neuronal stem cells in the SVZ give rise to astrocytes (a mesenchymal cell population similar to αSMA$^+$ cells), which differentiate to groups of proliferating cells before joining the rostral migratory stream (Fuentealba et al., 2012). The cardiac renewal process is also confined to a small subpopulation of mature CMs, similar to what is observed in the adult brain, where renewal is mainly restricted to the olfactory bulb and dentate gyrus.

Our data indicate that ECs, through the process of EndMT, are capable of generating cells with CSC characteristics in the uninjured adult heart. Other investigators and we have shown that TGF-β/BMP and Wnt signaling pathways regulate EndMT after injury, and it is likely that these pathways also regulate the

process during homeostasis (Zeisberg et al., 2007; Aisagbonhi et al., 2011; Chen et al., 2012). In addition, Sonic hedgehog signaling has been shown to activate Sca1$^+$ cells that have stem cell properties and reside in the adventitia layer of the arterial wall, and may also influence cardiogenic EC fate (Passman et al., 2008). The mechanisms that direct trafficking of the endothelial-derived cardiac progenitors remain to be determined. It is possible that A cells enter the circulation and are recruited to distal heart areas by chemokines such as SDF-1, similarly to mesenchymal stem cells (Wynn et al., 2004; Laird et al., 2008). Alternatively, local gradients of chemoattractants may recruit cells from their niche.

It is intriguing that adult ECs can give rise to myofibroblasts after cardiac injury (Zeisberg et al., 2007; Aisagbonhi et al., 2011). The striking parallels regarding the origins of CSCs and myofibroblasts raise the possibility the two processes are intrinsically linked. Thus, EC-derived CSCs may switch to a profibrotic phenotype in the disease environment after injury and alter their differentiation from CMs to myofibroblasts to preserve ventricular integrity. This scenario is reminiscent of the situation in skeletal muscle, where myoblasts switch from a regenerative to a profibrotic phenotype with aging (Brack et al., 2007). The ability of endogenous cardiac cells to change their fate based on their environment is further supported by a recent exciting finding that after cardiac injury, murine cardiac fibroblasts can be reprogrammed in vivo into CMs (Qian et al., 2012).

Our results also show that EC-derived CMs represent a small fraction of the total cardiac cell pool and are confined to specific areas. The first observation probably reflects the slow rate of cardiac renewal that is necessary during cardiac homeostasis, as evidenced by the low number of new CMs that are generated annually in human and mouse hearts (Bergmann et al., 2009; Murry and Lee, 2009). The second observation suggests that renewal may take place in specific sites characterized by high attrition rates due to work overload or structural constrains. In support of this possibility, clinical studies showed that cardiac tissue fibrosis often appears in the perivascular space or the insertion points between ventricles (Biernacka and Frangogiannis, 2011; Karamitsos and Neubauer, 2013), sites that contain many of the labeled clusters we identified in the mouse hearts.

Our model may also provide novel insights into how coronary arterial disease can lead to heart failure. It is likely that inflammation, oxidative stress, ischemia, calcification, and fibrosis around coronary vessels negatively impact the niche environment, disturbing the normal proliferation and differentiation of CSCs. This effect could compromise cardiac homeostasis, weaken the heart muscle, and eventually lead to hypertrophy and remodeling. Therefore, our findings may present novel opportunities to establish intrinsic cardiac molecular mechanisms and identify factors that prevent a profibrotic fate switch after injury in favor of cardiac regeneration.

EXPERIMENTAL PROCEDURES

Animals

ECs and their progeny were genetically labeled using Cre-LoxP recombination tools to activate expression of β-gal or various fluorescent proteins under the control of the ubiquitously active *ROSA* gene locus (Soriano, 1999). Three independent transgenic mouse lines were used to direct constitutive or inducible Cre recombinase activity specifically in ECs: the Tie1-Cre and VE-Cadherin-Cre lines (Gustafsson et al. 2001; Alva et al., 2006) and the endothelial-SCL-Cre-ER^T line, which drives a tamoxifen-inducible Cre-ER^T recombinase under control of the 5′ endothelial-specific enhancer of the *SCL* gene locus (Göthert et al., 2004). The EC-specific Cre lines were crossed to R26R*stopLacZ* (Soriano, 1999) or R26R*stopYFP* (Srinivas et al., 2001) mice to generate double transgenics. The Tie1-Cre mouse line was also bred with the multifluorescent reporter R26R*stopConfetti* (Snippert et al., 2010). Finally, transgenic mice expressing *β-gal* directly under the Tie1 promoter (Korhonen et al., 1995) were used to assess Tie1 expression in cardiac tissue. All animal experiments were approved by the Vanderbilt University Institutional Animal Care and Use Committee.

Whole-Mount β-Gal Activity Staining Assay

Whole mouse hearts were isolated into cold 1× PBS and fixed for 1 hr at 4°C in 1× PBS containing 2% paraformaldehyde (PFA). After fixation, the hearts were washed thrice with 1× PBS for 15 min each and kept overnight (O/N) at 30°C in X-gal staining solution (1 mg/ml X-gal, 5 mM potassium ferro- and ferricyanate, 2 mM magnesium chloride, and 0.02% NP-40 in 1× PBS). Whole-mount hearts were photographed, stored in 10% phosphate-buffered formalin at room temperature (RT) O/N and embedded in paraffin for sectioning.

Immuno- and Epifluorescence

For cryosectioning, freshly isolated hearts were perfused with 1× PBS, bisected transversely, and fixed in 4% PFA dissolved in 1× PBS for 2 hr at RT. The hearts were rinsed thrice in 0.1% TX-100 solution in 1× PBS for 5 min each, embedded in Optimal Cutting Temperature compound (OCT; VWR), sectioned, and stored at −70°C. Slides were thawed at RT and rehydrated in 1× PBS for 30 min to remove the OCT. Sections were washed twice in 0.1% TX-100 solution for 3 min each and permeabilized in 0.5% TX-100 solution for 20 min at RT. The sections were then blocked in 0.1% TX-100 solution containing 2% BSA and 10% normal goat serum (Sigma) for 30 min at RT, and incubated with primary antibodies O/N at 4°C. Afterward, the slides were washed four times in 1× PBS for 10 min each, incubated with secondary antibodies in blocking solution for 1 hr at RT, washed four times in 1× PBS for 10 min each, and mounted with VECTASHIELD fluorescent mounting medium (Vector Laboratories). Antibody sources and dilutions are described in Supplemental Experimental Procedures.

Imaging and 3D Reconstruction

A series of confocal images (z stack) were acquired sequentially on 100 μm cardiac sections. Image stacks were attained for each channel using an LSM 710 META inverted microscope (Zeiss). Images were maximally projected using ZEN or ImageJ software and reconstructed into 3D Z series using Imaris (Bitplane) image analysis software.

Quantification of Endothelial-Derived CMs per Volume of Cardiac Tissue in Pulse-Chase Experiments

Cardiac cross-sections from End-SCL-CreER^T-LacZ mice were stained with X-gal for β-gal activity and counterstained with hematoxylin and eosin (H&E), and then analyzed to determine the number of labeled CMs per volume of cardiac tissue. Transverse cardiac sections were imaged (Nikon AZ-100M widefield) and the average area was calculated using the Region Measurements function of MetaMorph image analysis software. The μm/pixel calibration value was used to convert pixels into area of tissue in μm^2. The volume of total cardiac tissue in μm^3 was calculated by multiplying the area obtained per section by the 10 μm thickness of tissue for each slide. A total of 352 slides (with four separate sections per slide, for a total of 1,408 sections) were imaged to analyze and estimate global cardiac CM labeling in the End-SCL-CreER^T-LacZ pulse-chase lineage tracing experiments (n = 17 mice).

Statistical Analysis

All values were reported as mean ± SD. Statistical significance was assessed by Student's unpaired two-tailed t test for all statistical analysis comparisons. Statistical significance was expressed as follows: *$p < 0.05$, **$p < 0.01$.

SUPPLEMENTAL INFORMATION

Supplemental Information includes Supplemental Experimental Procedures and six figures and can be found with this article online at http://dx.doi.org/10.1016/j.celrep.2014.06.004.

AUTHOR CONTRIBUTIONS

B.A.F. performed all experiments and wrote the manuscript. J.D.H. and D.T.P. helped with tissue section staining, imaging, and quantification. A.K.H. supervised experiments and wrote the manuscript.

ACKNOWLEDGMENTS

We thank Drs. H. Scott Baldwin, Douglas Sawyer, Chris Brown, Joey Barnett, and Ela Knapik for stimulating discussions, technical help, and generously sharing tools. We are indebted to Dr. David Harrison and Jing Wu for generously providing hearts from mice engrafted with fluorescently labeled bone marrow. We also thank Drs. Bryan Shepherd and Chun Li (Department of Biostatistics, Vanderbilt University) for assistance with statistical analyses. This work was supported by NIH grants U01HL100398 and R01HL083958 to A.K.H., a Training in Pharmacological Sciences fellowship (T32GM007628) and an American Heart Association predoctoral fellowship (11PRE7600210) to B.A.F., a Program in Cardiovascular Mechanisms: Training in Investigation fellowship (T32HL007411) to D.T.P., and the HHMI/VUMC Certificate Program in Molecular Medicine (B.A.F. and D.T.P.).

Received: January 15, 2014
Revised: April 21, 2014
Accepted: June 4, 2014
Published: July 3, 2014

REFERENCES

Adler, C.P., Friedburg, H., Herget, G.W., Neuburger, M., and Schwalb, H. (1996). Variability of cardiomyocyte DNA content, ploidy level and nuclear number in mammalian hearts. Virchows Arch. *429*, 159–164.

Aisagbonhi, O., Rai, M., Ryzhov, S., Atria, N., Feoktistov, I., and Hatzopoulos, A.K. (2011). Experimental myocardial infarction triggers canonical Wnt signaling and endothelial-to-mesenchymal transition. Dis. Model. Mech. *4*, 469–483.

Alva, J.A., Zovein, A.C., Monvoisin, A., Murphy, T., Salazar, A., Harvey, N.L., Carmeliet, P., and Iruela-Arispe, M.L. (2006). VE-Cadherin-Cre-recombinase transgenic mouse: a tool for lineage analysis and gene deletion in endothelial cells. Dev. Dyn. *235*, 759–767.

Anversa, P., Kajstura, J., Leri, A., and Bolli, R. (2006). Life and death of cardiac stem cells: a paradigm shift in cardiac biology. Circulation *113*, 1451–1463.

Arciniegas, E., Frid, M.G., Douglas, I.S., and Stenmark, K.R. (2007). Perspectives on endothelial-to-mesenchymal transition: potential contribution to vascular remodeling in chronic pulmonary hypertension. Am. J. Physiol. Lung Cell. Mol. Physiol. *293*, L1–L8.

Bearzi, C., Leri, A., Lo Monaco, F., Rota, M., Gonzalez, A., Hosoda, T., Pepe, M., Qanud, K., Ojaimi, C., Bardelli, S., et al. (2009). Identification of a coronary vascular progenitor cell in the human heart. Proc. Natl. Acad. Sci. USA *106*, 15885–15890.

Beltrami, A.P., Barlucchi, L., Torella, D., Baker, M., Limana, F., Chimenti, S., Kasahara, H., Rota, M., Musso, E., Urbanek, K., et al. (2003). Adult cardiac stem cells are multipotent and support myocardial regeneration. Cell *114*, 763–776.

Bergmann, O., Bhardwaj, R.D., Bernard, S., Zdunek, S., Barnabé-Heider, F., Walsh, S., Zupicich, J., Alkass, K., Buchholz, B.A., Druid, H., et al. (2009). Evidence for cardiomyocyte renewal in humans. Science *324*, 98–102.

Biernacka, A., and Frangogiannis, N.G. (2011). Aging and cardiac fibrosis. Aging Dis. *2*, 158–173.

Boudoulas, K.D., and Hatzopoulos, A.K. (2009). Cardiac repair and regeneration: the Rubik's cube of cell therapy for heart disease. Dis. Model. Mech. *2*, 344–358.

Bowman, A.N., van Amerongen, R., Palmer, T.D., and Nusse, R. (2013). Lineage tracing with Axin2 reveals distinct developmental and adult populations of Wnt/β-catenin-responsive neural stem cells. Proc. Natl. Acad. Sci. USA *110*, 7324–7329.

Brack, A.S., Conboy, M.J., Roy, S., Lee, M., Kuo, C.J., Keller, C., and Rando, T.A. (2007). Increased Wnt signaling during aging alters muscle stem cell fate and increases fibrosis. Science *317*, 807–810.

Chen, P.-Y., Qin, L., Barnes, C., Charisse, K., Yi, T., Zhang, X., Ali, R., Medina, P.P., Yu, J., Slack, F.J., et al. (2012). FGF regulates TGF-β signaling and endothelial-to-mesenchymal transition via control of let-7 miRNA expression. Cell Reports *2*, 1684–1696.

Dey, D., Han, L., Bauer, M., Sanada, F., Oikonomopoulos, A., Hosoda, T., Unno, K., De Almeida, P., Leri, A., and Wu, J.C. (2013). Dissecting the molecular relationship among various cardiogenic progenitor cells. Circ. Res. *112*, 1253–1262.

Doevendans, P.A., Daemen, M.J., de Muinck, E.D., and Smits, J.F. (1998). Cardiovascular phenotyping in mice. Cardiovasc. Res. *39*, 34–49.

Domínguez, D., Montserrat-Sentís, B., Virgós-Soler, A., Guaita, S., Grueso, J., Porta, M., Puig, I., Baulida, J., Francí, C., and García de Herreros, A. (2003). Phosphorylation regulates the subcellular location and activity of the snail transcriptional repressor. Mol. Cell. Biol. *23*, 5078–5089.

Ellison, G.M., Torella, D., Karakikes, I., and Nadal-Ginard, B. (2007). Myocyte death and renewal: modern concepts of cardiac cellular homeostasis. Nat. Clin. Pract. Cardiovasc. Med. *4* (*Suppl 1*), S52–S59.

Ellison, G.M., Vicinanza, C., Smith, A.J., Aquila, I., Leone, A., Waring, C.D., Henning, B.J., Stirparo, G.G., Papait, R., Scarfò, M., et al. (2013). Adult c-kit(pos) cardiac stem cells are necessary and sufficient for functional cardiac regeneration and repair. Cell *154*, 827–842.

Fioret, B.A., and Hatzopoulos, A.K. (2014). Comparative analysis of adult stem cell niches. In Chemical Biology in Regenerative Medicine: Bridging Stem Cells and Future Therapies, A. Ao, J. Hao, and C. Hong, eds. (Chichester, UK: Wiley-The Atrium, Southern Gate).

Fuentealba, L.C., Obernier, K., and Alvarez-Buylla, A. (2012). Adult neural stem cells bridge their niche. Cell Stem Cell *10*, 698–708.

Göthert, J.R., Gustin, S.E., van Eekelen, J.A.M., Schmidt, U., Hall, M.A., Jane, S.M., Green, A.R., Göttgens, B., Izon, D.J., and Begley, C.G. (2004). Genetically tagging endothelial cells in vivo: bone marrow-derived cells do not contribute to tumor endothelium. Blood *104*, 1769–1777.

Greif, D.M., Kumar, M., Lighthouse, J.K., Hum, J., An, A., Ding, L., Red-Horse, K., Espinoza, F.H., Olson, L., Offermanns, S., and Krasnow, M.A. (2012). Radial construction of an arterial wall. Dev. Cell *23*, 482–493.

Gustafsson, E., Brakebusch, C., Hietanen, K., and Fässler, R. (2001). Tie-1-directed expression of Cre recombinase in endothelial cells of embryoid bodies and transgenic mice. J. Cell Sci. *114*, 671–676.

Hierlihy, A.M., Seale, P., Lobe, C.G., Rudnicki, M.A., and Megeney, L.A. (2002). The post-natal heart contains a myocardial stem cell population. FEBS Lett. *530*, 239–243.

Karamitsos, T.D., and Neubauer, S. (2013). The prognostic value of late gadolinium enhancement CMR in nonischemic cardiomyopathies. Curr. Cardiol. Rep. *15*, 326.

Kattman, S.J., Huber, T.L., and Keller, G.M. (2006). Multipotent flk-1+ cardiovascular progenitor cells give rise to the cardiomyocyte, endothelial, and vascular smooth muscle lineages. Dev. Cell *11*, 723–732.

Kopinke, D., Brailsford, M., Shea, J.E., Leavitt, R., Scaife, C.L., and Murtaugh, L.C. (2011). Lineage tracing reveals the dynamic contribution of Hes1+ cells to the developing and adult pancreas. Development *138*, 431–441.

Korhonen, J., Lahtinen, I., Halmekytö, M., Alhonen, L., Jänne, J., Dumont, D., and Alitalo, K. (1995). Endothelial-specific gene expression directed by the tie gene promoter in vivo. Blood *86*, 1828–1835.

Laird, D.J., von Andrian, U.H., and Wagers, A.J. (2008). Stem cell trafficking in tissue development, growth, and disease. Cell *132*, 612–630.

Lancrin, C., Sroczynska, P., Stephenson, C., Allen, T., Kouskoff, V., and Lacaud, G. (2009). The haemangioblast generates haematopoietic cells through a haemogenic endothelium stage. Nature *457*, 892–895.

Li, L., and Clevers, H. (2010). Coexistence of quiescent and active adult stem cells in mammals. Science *327*, 542–545.

Malliaras, K., Zhang, Y., Seinfeld, J., Galang, G., Tseliou, E., Cheng, K., Sun, B., Aminzadeh, M., and Marbán, E. (2013). Cardiomyocyte proliferation and progenitor cell recruitment underlie therapeutic regeneration after myocardial infarction in the adult mouse heart. EMBO Mol. Med. *5*, 191–209.

Martin, C.M., Meeson, A.P., Robertson, S.M., Hawke, T.J., Richardson, J.A., Bates, S., Goetsch, S.C., Gallardo, T.D., and Garry, D.J. (2004). Persistent expression of the ATP-binding cassette transporter, Abcg2, identifies cardiac SP cells in the developing and adult heart. Dev. Biol. *265*, 262–275.

Medici, D., Shore, E.M., Lounev, V.Y., Kaplan, F.S., Kalluri, R., and Olsen, B.R. (2010). Conversion of vascular endothelial cells into multipotent stem-like cells. Nat. Med. *16*, 1400–1406.

Messina, E., De Angelis, L., Frati, G., Morrone, S., Chimenti, S., Fiordaliso, F., Salio, M., Battaglia, M., Latronico, M.V.G., Coletta, M., et al. (2004). Isolation and expansion of adult cardiac stem cells from human and murine heart. Circ. Res. *95*, 911–921.

Mouquet, F., Pfister, O., Jain, M., Oikonomopoulos, A., Ngoy, S., Summer, R., Fine, A., and Liao, R. (2005). Restoration of cardiac progenitor cells after myocardial infarction by self-proliferation and selective homing of bone marrow-derived stem cells. Circ. Res. *97*, 1090–1092.

Murry, C.E., and Lee, R.T. (2009). Development biology. Turnover after the fallout. Science *324*, 47–48.

Murry, C.E., Soonpaa, M.H., Reinecke, H., Nakajima, H., Nakajima, H.O., Rubart, M., Pasumarthi, K.B., Virag, J.I., Bartelmez, S.H., Poppa, V., et al. (2004). Haematopoietic stem cells do not transdifferentiate into cardiac myocytes in myocardial infarcts. Nature *428*, 664–668.

Oh, H., Bradfute, S.B., Gallardo, T.D., Nakamura, T., Gaussin, V., Mishina, Y., Pocius, J., Michael, L.H., Behringer, R.R., Garry, D.J., et al. (2003). Cardiac progenitor cells from adult myocardium: homing, differentiation, and fusion after infarction. Proc. Natl. Acad. Sci. USA *100*, 12313–12318.

Passman, J.N., Dong, X.R., Wu, S.P., Maguire, C.T., Hogan, K.A., Bautch, V.L., and Majesky, M.W. (2008). A sonic hedgehog signaling domain in the arterial adventitia supports resident Sca1+ smooth muscle progenitor cells. Proc. Natl. Acad. Sci. USA *105*, 9349–9354.

Pfister, O., Mouquet, F., Jain, M., Summer, R., Helmes, M., Fine, A., Colucci, W.S., and Liao, R. (2005). CD31− but not CD31+ cardiac side population cells exhibit functional cardiomyogenic differentiation. Circ. Res. *97*, 52–61.

Qian, L., Huang, Y., Spencer, C.I., Foley, A., Vedantham, V., Liu, L., Conway, S.J., Fu, J.D., and Srivastava, D. (2012). In vivo reprogramming of murine cardiac fibroblasts into induced cardiomyocytes. Nature *485*, 593–598.

Rota, M., Padin-Iruegas, M.E., Misao, Y., De Angelis, A., Maestroni, S., Ferreira-Martins, J., Fiumana, E., Rastaldo, R., Arcarese, M.L., Mitchell, T.S., et al. (2008). Local activation or implantation of cardiac progenitor cells rescues scarred infarcted myocardium improving cardiac function. Circ. Res. *103*, 107–116.

Senyo, S.E., Steinhauser, M.L., Pizzimenti, C.L., Yang, V.K., Cai, L., Wang, M., Wu, T.-D., Guerquin-Kern, J.-L., Lechene, C.P., and Lee, R.T. (2013). Mammalian heart renewal by pre-existing cardiomyocytes. Nature *493*, 433–436.

Smith, R.R., Barile, L., Cho, H.C., Leppo, M.K., Hare, J.M., Messina, E., Giacomello, A., Abraham, M.R., and Marbán, E. (2007). Regenerative potential of cardiosphere-derived cells expanded from percutaneous endomyocardial biopsy specimens. Circulation *115*, 896–908.

Snippert, H.J., van der Flier, L.G., Sato, T., van Es, J.H., van den Born, M., Kroon-Veenboer, C., Barker, N., Klein, A.M., van Rheenen, J., Simons, B.D., and Clevers, H. (2010). Intestinal crypt homeostasis results from neutral competition between symmetrically dividing Lgr5 stem cells. Cell *143*, 134–144.

Soriano, P. (1999). Generalized lacZ expression with the ROSA26 Cre reporter strain. Nat. Genet. *21*, 70–71.

Srinivas, S., Watanabe, T., Lin, C.-S., William, C.M., Tanabe, Y., Jessell, T.M., and Costantini, F. (2001). Cre reporter strains produced by targeted insertion of EYFP and ECFP into the ROSA26 locus. BMC Dev. Biol. *1*, 4.

Timmerman, L.A., Grego-Bessa, J., Raya, A., Bertrán, E., Pérez-Pomares, J.M., Díez, J., Aranda, S., Palomo, S., McCormick, F., Izpisúa-Belmonte, J.C., and de la Pompa, J.L. (2004). Notch promotes epithelial-mesenchymal transition during cardiac development and oncogenic transformation. Genes Dev. *18*, 99–115.

Uchida, S., De Gaspari, P., Kostin, S., Jenniches, K., Kilic, A., Izumiya, Y., Shiojima, I., Grosse Kreymborg, K., Renz, H., Walsh, K., and Braun, T. (2013). Sca1-derived cells are a source of myocardial renewal in the murine adult heart. Stem Cell Rep. *1*, 397–410.

Van Handel, B., Montel-Hagen, A., Sasidharan, R., Nakano, H., Ferrari, R., Boogerd, C.J., Schredelseker, J., Wang, Y., Hunter, S., Org, T., et al. (2012). Scl represses cardiomyogenesis in prospective hemogenic endothelium and endocardium. Cell *150*, 590–605.

Wang, X., Hu, Q., Nakamura, Y., Lee, J., Zhang, G., From, A.H.L., and Zhang, J. (2006). The role of the sca-1+/CD31- cardiac progenitor cell population in postinfarction left ventricular remodeling. Stem Cells *24*, 1779–1788.

Wynn, R.F., Hart, C.A., Corradi-Perini, C., O'Neill, L., Evans, C.A., Wraith, J.E., Fairbairn, L.J., and Bellantuono, I. (2004). A small proportion of mesenchymal stem cells strongly expresses functionally active CXCR4 receptor capable of promoting migration to bone marrow. Blood *104*, 2643–2645.

Zeisberg, E.M., Tarnavski, O., Zeisberg, M., Dorfman, A.L., McMullen, J.R., Gustafsson, E., Chandraker, A., Yuan, X., Pu, W.T., Roberts, A.B., et al. (2007). Endothelial-to-mesenchymal transition contributes to cardiac fibrosis. Nat. Med. *13*, 952–961.

Zeisberg, E.M., Potenta, S.E., Sugimoto, H., Zeisberg, M., and Kalluri, R. (2008). Fibroblasts in kidney fibrosis emerge via endothelial-to-mesenchymal transition. J. Am. Soc. Nephrol. *19*, 2282–2287.